Electronic Supplementary Information

Ordered Mesoporous Silica/Polyvinylidene Fluoride Composite Membranes with Three-Dimensional Interpenetrating Structure for Efficient Removal of Water Contaminants

Jianwei Fan,[a] Dandan Li,[a] Wei Teng,[a] Jianping Yang,[a] Yong Liu,[b] Liangliang Liu,[b] Ahmed A. Elzatahry,[d] Abdulaziz Alghamdi,[e] Yonghui Deng,*[b,c] Guangming Li,[a] Wei-xian Zhang,[a] and Dongyuan Zhao[b]

[a] College of Environmental Science and Engineering, Tongji University, and State Key Laboratory of Pollution Control and Resource Reuse, Shanghai 200092, China

[b] Department of Chemistry and Shanghai Key Laboratory of Molecular Catalysis and Innovative Materials, State Key Laboratory of Molecular Engineering of Polymers, Fudan University, Shanghai 200433, China

[c] State Key Lab of Transducer Technology, Shanghai Institute of Microsystem and Information Technology, Chinese Academy of Sciences, Shanghai 200050, China.

[d] College of Arts and Sciences, Qatar University, PO Box 2713, Doha, Qatar.

[e] Department of Chemistry, College of Science, King Saud University, Riyadh 11451, Saudi Arabia Materials Science and Technology Program.

SI Figures

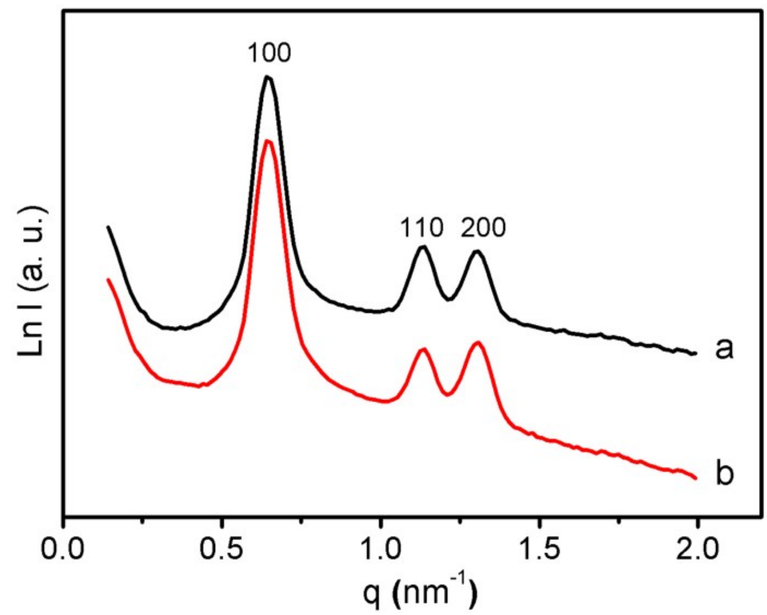

Figure S1. SAXS patterns of the a) pristine ordered mesoporous silica (OMS) and the b) amino-group functionalized ordered mesoporous silica (OMS-NH_2)

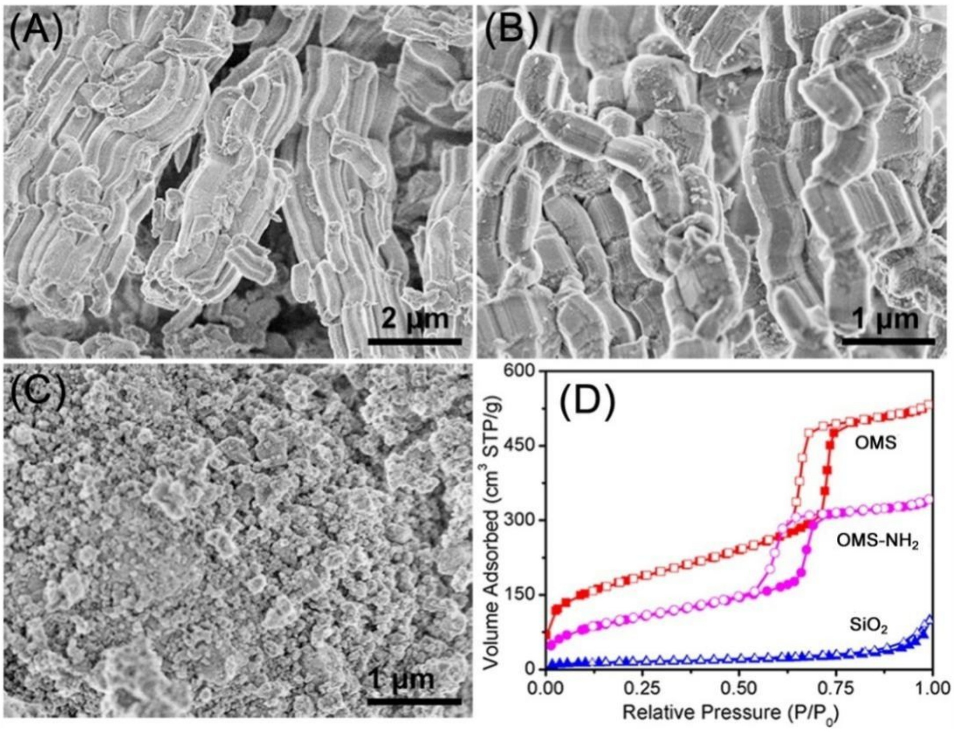

Figure S2. SEM images of A) the pristine ordered mesoporous silica (OMS), B) amino-functionalized ordered mesoporous silica (OMS-NH_2), and C) commercial SiO_2. D) N_2 sorption isotherms of the OMS, OMS-NH_2, and commercial SiO_2

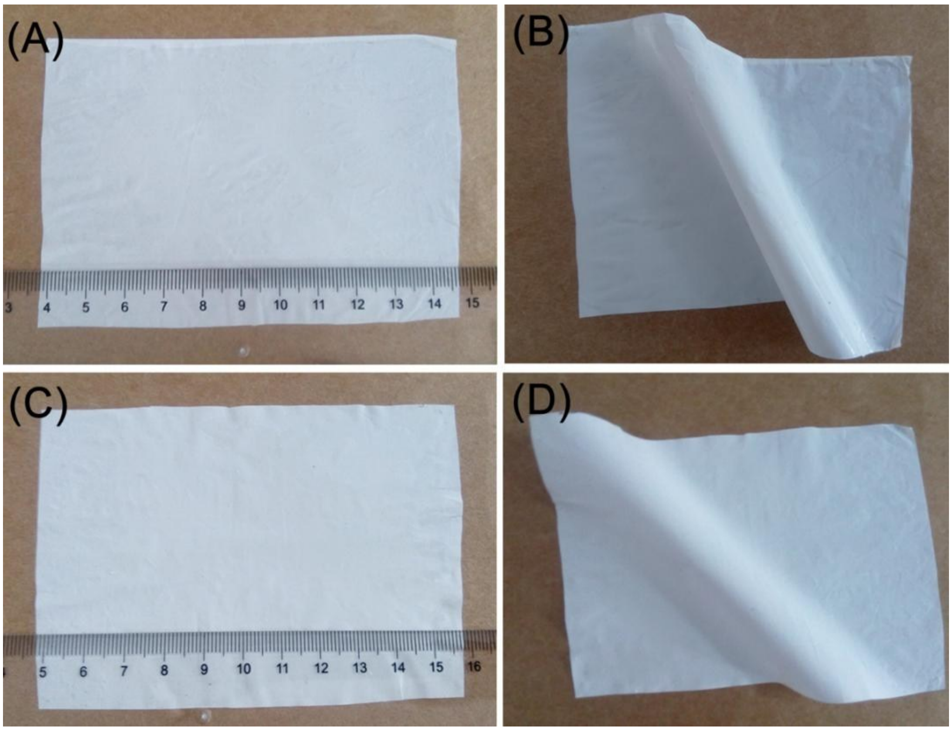

Figure S3. Optical photographs of the pure PVDF membrane (A, B) and the OMS/PVDF-3 composite membrane (C, D).

The optical photographs of the pure PVDF (Figure S3A) and the OMS/PVDF-3 membranes (Figure S3C) show that both of the membranes are continuous and defect-free, exhibiting no apparent differences. Both of the membranes can be bended and folded easily without any brittle fractures (Figure S3B, D), suggesting a good flexibility of the membranes. In addition, sizes of the membranes can be controlled easily by adjusting the scraper length of the film applicator during the casting process, confirming that the one-step non-solvent induced phase separation method is facile and feasible for the membrane fabrication.

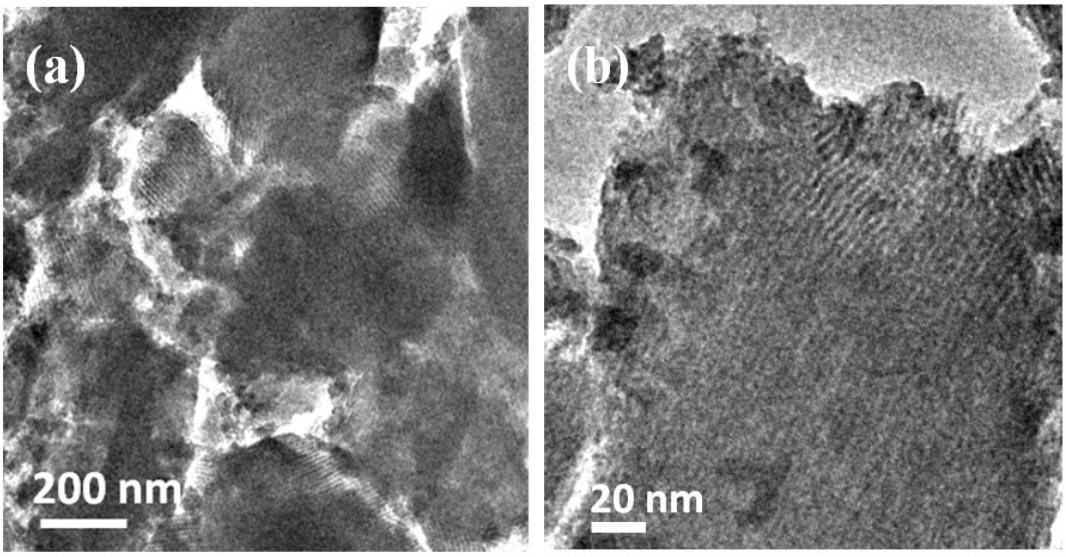

Figure S4. TEM images (a, b) of the composite membrane OMS/PVDF-3. Before the TEM measurement, the sample was submitted to ultrathin microtomming, and the collected pieces were used for TEM observation

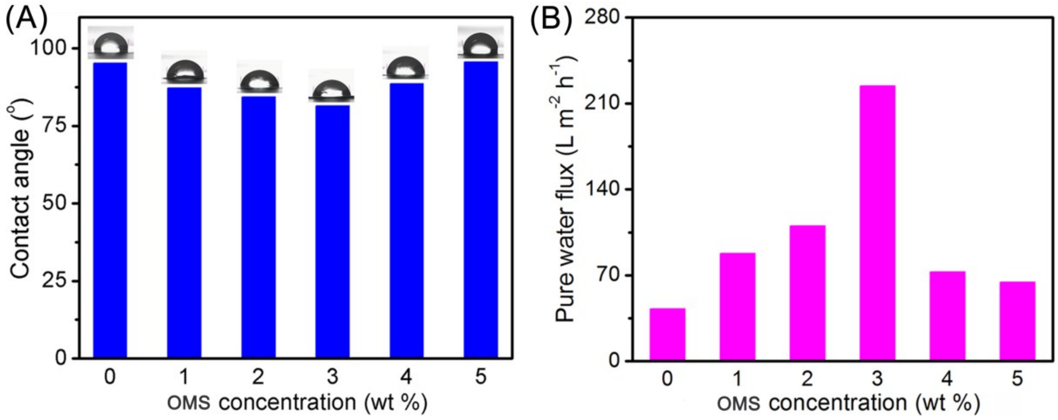

Figure S5. Effects of the OMS concentrations in the casting solution on (A) static water contact angles of the membrane surfaces and (B) water flux of the obtained membranes

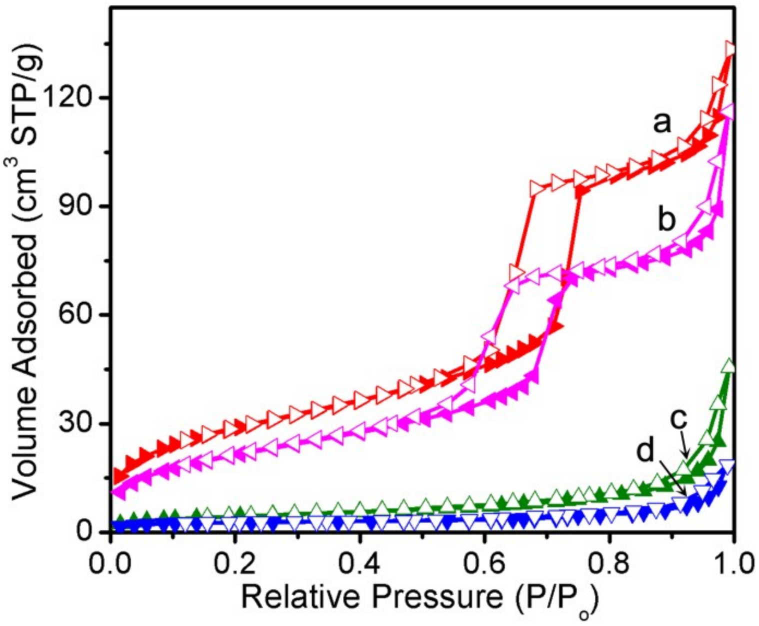

Figure S6. N_2 sorption isotherms of a) the OMS/PVDF-3 membrane, b) OMS-NH_2/PVDF-3 membrane, c) SiO_2/PVDF-3 membrane, and d) the pure PVDF membrane. The adsorption curves and desorption curves are indicated by filled symbols and open symbols, respectively.

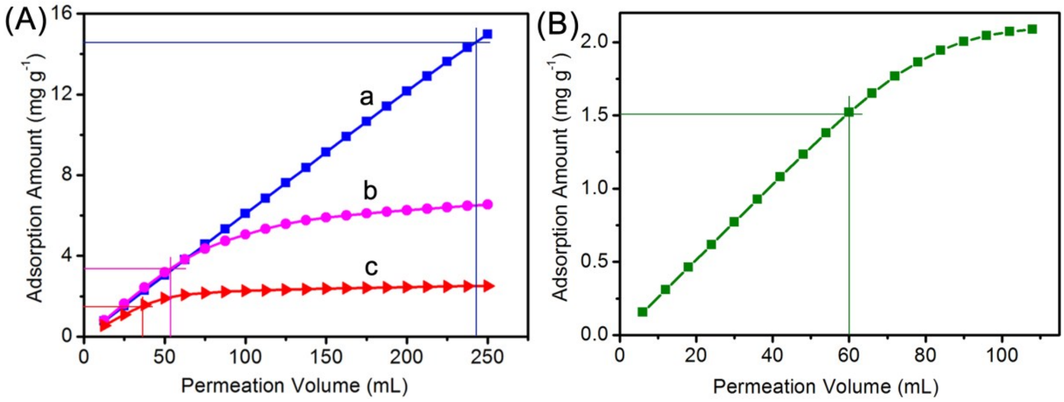

Figure S7. (A) Dynamic adsorption amounts for methylene blue by a) the OMS/PVDF-3 membrane, b) SiO_2/PVDF-3 membrane, and c) pure PVDF membrane, at a flow rate of 98.7 L m^{-2} h^{-1}. The dynamic adsorption tests were carried out with a feed concentration of 5.0 mg L^{-1}. (B) Dynamic adsorption amount for Cu (II) ions by the OMS-NH_2/PVDF-3 membrane, at a flow rate of 39.4 L m^{-2} h^{-1}. The dynamic adsorption test was carried out with a feed concentration of 2.0 mg L^{-1}.

SI Tables

Table S1. Structural and textural parameters of the ordered mesoporous silica (SBA-15) and MS and OMS-NH_2 obtained by modifying SBA-15 with 3-aminopropyltriethoxysilane

Mesoporous fillers	S_{BET} (m^2 g^{-1}) [a]	V_t (cm^3 g^{-1}) [b]	D (nm) [c]
OMS	686	0.79	6.30
OMS-NH_2	367	0.48	5.86

[a] surface area calculated by BET method;

[b] pore volume calculated by BJH method from the adsorption branch of isotherms;

[c] average pore diameter of the mesoporous fillers.

Table S2. The porosity, static water contact angles, and water fluxes of the obtained membranes with different contents of OMS.

OMS contents in the casting solution (wt %)	Porosity of the obtained membranes (%)	Contact angles of the obtained membranes (°)	Water fluxes of the obtained membranes (L m^{-2} h^{-1})
0	65.0	95.3	42.6
1	69.3	87.2	87.9
2	70.8	84.4	110.3
3	72.3	81.5	224.5
4	73.0	88.6	72.9
5	74.3	95.6	64.5

Table S3. BET surface areas and dynamic adsorption of the membranes and fillers.

Membranes	BET surface area ($m^2 g^{-1}$)	Inorganic fillers	BET surface area ($m^2 g^{-1}$)	Dynamic adsorption capacity for MB (mg g^{-1})	Dynamic adsorption capacity for Cu(II) ions (mg g^{-1})
OMS/PVDF-3	105	OMS	686	14.5	~ 0
OMS-NH_2/PVDF-3	76	OMS-NH_2	367	—	1.5
SiO_2/PVDF-3	16	Commercial SiO_2	51	3.3	—
Neat PVDF	10	—	—	1.5	—